Structure
Article

Design of a bZip Transcription Factor with Homo/Heterodimer-Induced DNA-Binding Preference

Vivian Pogenberg,[1,6] Larissa Consani Textor,[1,6] Laurent Vanhille,[2,3,4,6] Simon J. Holton,[1,7] Michael H. Sieweke,[2,3,4,5] and Matthias Wilmanns[1,*]
[1]EMBL Hamburg c/o DESY, Notkestraße 85, 22603 Hamburg, Germany
[2]Centre d'Immunologie de Marseille-Luminy (CIML), Aix-Marseille Université, UM2, Campus de Luminy, Case 906, 13288 Marseille Cedex 09, France
[3]Institut National de la Santé et de la Recherche Médicale (INSERM), U1104, Marseille, France
[4]Centre National de la Recherche Scientifique (CNRS), UMR7280, Marseille, France
[5]Max-Delbrück-Centrum für Molekulare Medizin (MDC), Robert-Rössle-Straße 10, 13125 Berlin, Germany
[6]These authors contributed equally to this work
[7]Present address: Structural Biology/Lead Discovery, Bayer Pharmaceuticals, 13342 Berlin, Germany
*Correspondence: wilmanns@embl-hamburg.de
http://dx.doi.org/10.1016/j.str.2013.12.017

SUMMARY

The ability of basic leucine zipper transcription factors for homo- or heterodimerization provides a paradigm for combinatorial control of eukaryotic gene expression. It has been unclear, however, how facultative dimerization results in alternative DNA-binding repertoires on distinct regulatory elements. To unravel the molecular basis of such coupled preferences, we determined two high-resolution structures of the transcription factor MafB as a homodimer and as a heterodimer with c-Fos bound to variants of the Maf-recognition element. The structures revealed several unexpected and dimer-specific coiled-coil-heptad interactions. Based on these findings, we have engineered two MafB mutants with opposite dimerization preferences. One of them showed a strong preference for MafB/c-Fos heterodimerization and enabled selection of heterodimer-favoring over homodimer-specific Maf-recognition element variants. Our data provide a concept for transcription factor design to selectively activate dimer-specific pathways and binding repertoires.

INTRODUCTION

The transcription of genes is a highly regulated combinatorial process that is mediated by large and dynamic multicomponent protein assemblies such as the enhanceosome (Ogata et al., 2003; Panne, 2008; Reményi et al., 2004). These assemblies generally involve several distinct transcription factors that act as homo- or hetero-oligomeric assemblies on specific cis-regulatory DNA promoter and enhancer sites, ultimately modifying the local chromatin architecture to activate the polymerase II machinery on the target promoter site. Their ability to assemble with several alternative binding partners allows many transcription factors to be involved in the combinatorial transcription of different genes, leading to unrelated, sometimes even antagonistic, functional readouts or distinct cell fate decisions (Sieweke and Graf, 1998). Understanding the basic mechanisms of variable protein assembly in gene transcription is essential for the rationalization of genotypic and phenotypic effects during development and pathology. This knowledge of the underlying molecular parameters could ultimately be used to engineer altered transcription circuits.

An important example of such alternative transcription factor assemblies is the basic leucine zipper (bZip) transcription factor family, which binds to a variety of related cyclic AMP-response and 12-*O*-tetradecanoate-13-acetate-response element (CRE/TRE) DNA-recognition sites both as homo- or heterodimeric complexes (Miller, 2009). Their large combinatorial versatility is established by sequence-specific coiled coil assemblies within the long leucine zipper (Zip) segment, which is next to the basic region (BR) that functions as a direct DNA-binding segment. The molecular determinants of coiled-coil interactions in bZip transcription factors have been extensively studied by biophysical, structural, and computational approaches and engineering experiments (Grigoryan and Keating, 2008; Miller, 2009; Vinson et al., 2006). Available data, however, are limited to studies of bZip factors in the absence of DNA and using dimer pairs with similar DNA-binding preferences, such as members of the c-Jun/c-Fos family that have a common preference for CRE/TRE. In essence, these data indicate that typical leucine zipper interfaces are formed by hydrophobic knob-into-holes interactions of residues from heptad positions *a* and *d* and additional facultative electrostatic interactions between residues from positions *e* and *g*. Collectively, the absence/presence of suitable residues in those positions allowing the formation of these interactions is thought to govern specificity for the ability of assembling either into homo- or heterodimers with other bZip transcription factors. Since the overall arrangement in leucine zippers is structurally conserved, available experimental structural data have limited power to predict those interactions in related bZip transcription factor assemblies.

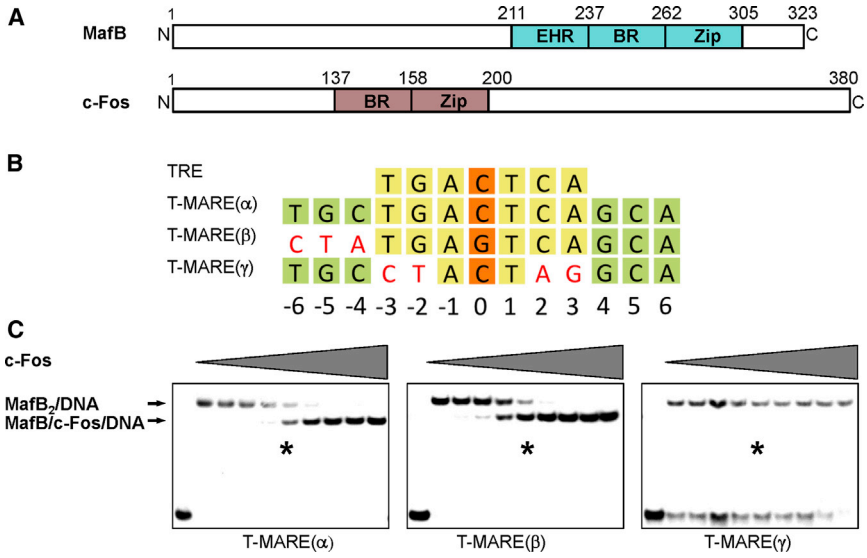

Figure 1. Binding of MafB/c-Fos to T-MARE Variants

(A) MafB and c-Fos constructs used for analysis, colored in cyan (MafB) and chocolate (c-Fos). The domain boundaries are indicated, as observed in the structures of the respective complexes (cf. Figure 2).

(B) Sequences of TRE, conventional T-MARE(α), and T-MARE variants (β and γ). Color codes: flanking MARE sequences (positions −6 to −4, +4 to +6), green; TRE (positions −3 to +3), yellow, except central position 0, orange; MARE(β, γ) mutations are indicated in red.

(C) EMSA of 4 pmol MafB in the presence of various concentrations (0.25, 0.5, 1, 2, 4, 8, 16, 32, and 64 pmol, from left to right, increasing concentrations indicated above) of c-Fos on T-MARE(α) (left panel), T-MARE(β) (center panel), and T-MARE(γ) (right panel). Equimolar concentration of MafB and c-Fos is indicated by asterisk.

However, a direct comparison of alternative bZip complexes with assembly-specific preferences for distinct DNA-recognition elements has not been performed and could identify the determinants of binding repertoire and target gene selection (Miller, 2009; Yamamoto et al., 2006). To investigate bZip assembly-dependent DNA-binding site selection, we have studied two prototype bZip transcription factors with different DNA-binding recognition sites and the ability to heterodimerize: MafB and c-Fos (Kataoka et al., 1994; Kerppola and Curran, 1994b; Newman and Keating, 2003). MafB plays important roles in tumorigenesis, differentiation, and several developmental processes such as hematopoiesis (Aziz et al., 2009; Eychène et al., 2008; Sarrazin et al., 2009; Tillmanns et al., 2007). In particular in macrophages, MafB is constitutively expressed, whereas c-Fos is transiently induced upon pathogen challenge or cytokine stimulation and has immunomodulatory functions in macrophages and dendritic cells (Amit et al., 2009; Introna et al., 1986; Koga et al., 2009; Pulendran et al., 2010). In terms of overall domain structure, MafB is a member of the Maf subfamily of bZip transcription factors, which share an additional helical bundle region, known as the extended homology region (EHR), preceding the BR (Kataoka et al., 1994; Kerppola and Curran, 1994a; Kusunoki et al., 2002; Figure 1A). MafB requires a long DNA-recognition sequence known as the Maf-recognition element (MARE) that includes a three-base extension of the central 7 or 8 bp CRE/TRE core motif of the canonical bZip recognition element (Yamamoto et al., 2006). Here we have focused on MARE sequences with a 7 bp TRE-type core (T-MARE; Figure 1B). Interestingly, MAREs that have been found in confirmed target genes are highly degenerate in both the TRE core motif and the two flanking regions (Yamamoto et al., 2006). The major reported heterodimeric bZip binding partner of MafB is c-Fos (Kataoka et al., 1994; Kerppola and Curran, 1994b; Newman and Keating, 2003) (Figure 1A). In contrast to MafB, c-Fos does not homodimerize and its specific DNA interactions are limited to the central CRE/TRE (Glover and Harrison, 1995; Hai and Curran, 1991), thus the presence of the flanking segments of the MARE are not required for c-Fos binding.

RESULTS AND DISCUSSION

Structure Determination of Distinct $MafB_2$ and MafB/c-Fos DNA Complexes

To determine the molecular parameters that govern specific binding of the homodimeric $MafB_2$ and heterodimeric MafB/c-Fos complexes to the T-MARE motif, we investigated T-MARE variants with an expected preference for the homodimeric $MafB_2$ or the heterodimeric MafB/c-Fos assembly. We used the following oligonucleotides (Figure 1B): (1) a canonical, palindromic T-MARE motif (5′-TGCTGACTCAGCA-3′) with an intact TRE site and two flanking MARE extensions (underlined), referred to as T-MARE(α); (2) an asymmetric oligonucleotide (5′-TGAGTCAGCA-3′) with only one MARE extension (underlined) flanking the central TRE, referred to as T-MARE(β), to promote MafB/c-Fos heterodimerization; and (3) a third oligonucleotide (5′-TGC*CTACTAG*GCA-3′) that has two unchanged MARE extensions and an altered TRE core motif (changes in italics), referred to as T-MARE(γ), to promote $MafB_2$ homodimerization.

As shown by an electrophoretic mobility shift assay (EMSA), at an equimolar ratio of MafB and c-Fos, both complexes—homodimeric $MafB_2$ and heterodimer MafB/c-Fos—are found at comparable concentrations when bound to T-MARE(α). Changing the ratio of the two transcription factors by c-Fos titration resulted in a shift in complex formation: homodimeric $MafB_2$ in the presence of excess MafB and heterodimeric MafB/c-Fos in the presence of excess c-Fos. Under identical experimental conditions, T-MARE(β) showed a strong preference for MafB/c-Fos, and T-MARE(γ) bound only homodimeric $MafB_2$ with no significant amount of heterodimeric MafB/c-Fos detected (Figure 1C).

Using a previously established purification protocol (Textor et al., 2007), we first determined the crystal structure of homodimeric $MafB_2$ with a 20 bp DNA duplex, encompassing the T-MARE motif, at 2.9 Å resolution (Table 1 and Figure 2A). To obtain a pure heterodimeric MafB/c-Fos complex suitable for crystallization, we exploited the established binding preference of heterodimeric MafB/c-Fos for T-MARE(β) (Figure 1C), allowing

Table 1. Data Collection, Phasing, and Refinement Statistics

	MafB/c-Fos/T-MARE(β)		$MafB_2$/T-MARE(α)
	Native	Iodine Derivatized	Native
Data Collection			
Space group	$P6_2$		$P22_12_1$
Cell dimensions			
a, *b*, *c* (Å)	146.7, 146.7, 51.2		41.2, 49.8, 170.4
Resolution (Å)	47.4–2.3 (2.42–2.3)[a]	64.0–3.2 (3.5–3.2)[a]	170.4–2.9 (3.0–2.9)[a]
R_{sym} or R_{merge}	5.2 (32.0)[a]	10.0 (19.9)[a]	9.8 (32.9)[a]
$I/\sigma I$	10.1 (2.4)[a]	6.1 (1.9)[a]	6.8 (2.2)[a]
Completeness (%)	99.5 (99.3)[a]	97.2 (81.4)[a]	100 (99.7)[a]
Redundancy	11.9 (10.2)[a]	42.3 (28.2)[a]	6.9 (6.6)[a]
Refinement			
Resolution (Å)	47.4–2.3		64.0–3.2
Reflections (n)	28,122		8,174
R_{work}/R_{free}	22.8/25.6		23.5/27.5
Atoms (n)			
Protein	1,329		1,588
DNA	650		799
Others	177		72
B-factors			
Protein	45.7		38.4
DNA	41.0		32.3
Others	45.6		31.9
Rmsd			
Bond lengths (Å)	0.009		0.007
Bond angles (°)	1.39		1.26

[a]Values in parentheses are for the highest-resolution shell.

the separation of a highly pure MafB/c-Fos/T-MARE(β) complex (Figure S1 available online) and its X-ray structure determination at 2.3 Å resolution.

In the homodimeric $MafB_2$/T-MARE complex, each MafB protomer symmetrically binds to one of the two T-MARE half-sites (Figure 2A). The two MafB molecules show a virtually identical overall conformation, reflected by a root-mean-squares deviation (rmsd) of 1.7 Å for 92 common residues. Based on this structure, we have defined three sequence segments for each MafB polypeptide chain (Figures 1A and 2A): the first represents the N-terminal EHR, which folds into a small three-helical bundle domain or helix-turn-helix motif (residues 211–237); the second sequence segment represents the BR that binds into the major groove of each T-MARE half-binding site (residues 238–261); the third segment forms the Zip region that establishes the homodimeric MafB assembly by a long, left-handed coiled coil (residues 262–305). The Zip and BR together constitute the basic zipper (bZip) region, which folds into a long, uninterrupted 75-residue helix with more than 20 helical turns.

In contrast to the $MafB_2$/T-MARE complex, the heterodimer MafB/c-Fos/T-MARE(β) complex is asymmetric, owing to the two different protein ligands (MafB, c-Fos) and the lack of one of the two MARE extensions in the DNA motif (Figure 2B). MafB is bound to the remaining T-MARE half-site, whereas c-Fos binds to the opposite TRE half-site without the T-MARE extension. Similarly to MafB, c-Fos comprises a BR (residues 137–160) involved in DNA binding, followed by the Zip segment (residues 161–200) that assembles with the equivalent MafB Zip segment (residues 262–301) into a heterodimeric coiled coil. In contrast to MafB, c-Fos does not comprise an additional EHR.

Recognition of Distinct MARE Variants by $MafB_2$ versus MafB/c-Fos

As we expected different DNA-binding preferences for MafB and c-Fos, we systematically analyzed the $MafB_2$/T-MARE and MafB/c-Fos/T-MARE(β) complexes in terms of the kind of molecular protein/DNA interactions observed in the two structures. Indeed, they revealed remarkable differences in the arrangement of the base-specific DNA interactions, formed with the central TRE motif and the flanking MARE nucleotides. In the structure of the heterodimeric MafB/c-Fos/T-MARE(β) complex, the observed protein-DNA interactions are highly asymmetric and are caused by mostly unrelated interactions from the two protein ligands (Figures 2B and 3). Most of the MafB-mediated interactions with the DNA half-site, which contain the remaining T-MARE extension, are identical to those found in the $MafB_2$/T-MARE complex (Figure S2). An exception is R256 from MafB that provides an additional base-specific interaction via a bidentate hydrogen bond pattern with guanine in the central position 0 of the heterodimeric

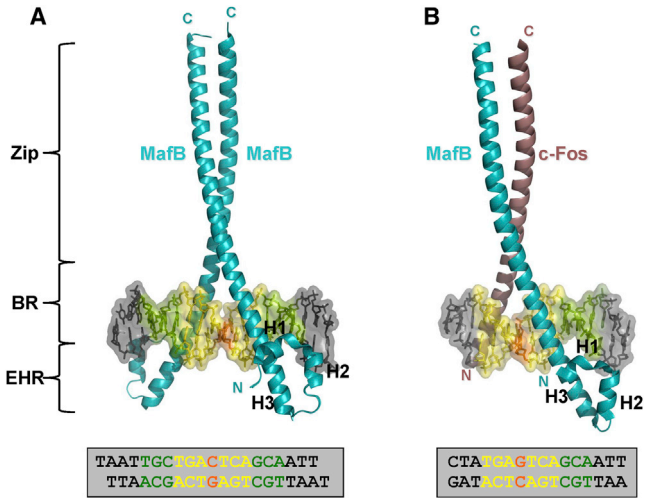

Figure 2. Overall Structure of $MafB_2$/T-MARE(α) and MafB/c-Fos/T-MARE(β) Complexes

Overall structure of (A) $MafB_2$/T-MARE(α) and (B) MafB/c-Fos/T-MARE(β) complexes. Color coding: MafB, cyan; c-Fos, chocolate; color codes of T-MARE(α)/T-MARE(β) are as in Figure 1. Protein structures are shown as ribbons, bound DNA is shown in combined stick and semitransparent surface representation. Protein structural segments (Zip, BR, EHR), helices of the EHR, and protein sequence termini are indicated. The T-MARE- and T-MARE(β)-containing oligonucleotide sequences used for crystallization are shown below, with color codes as in Figure 1.

MafB/c-Fos/T-MARE(β) complex (Figure 3). By contrast, the equivalent c-Fos residue (R155) is only involved in interactions with the DNA phosphate backbone. In addition, a total of six residues of the BR from c-Fos are involved in T-MARE(β) interactions that are mostly restricted to the central TRE of T-MARE(β). Only one c-Fos residue, N147, is involved in base-specific interactions by hydrogen bonds to C(+2) and T(−3), which are located on opposite strands within the same TRE half-site. N147 from c-Fos is structurally equivalent to N248 from MafB, which is one of two MafB key residues for base-specific interactions with T-MARE. Remarkably, a spatial difference of the asparagine side chain by about 2 Å is sufficient to allow different base-specific interactions either with the central TRE (mediated by c-Fos) or with the extended T-MARE (mediated by MafB; Figures 3C, 3D, and S2). The other c-Fos residue, R143, which has a conserved structural MafB equivalent involved in base-specific interactions (R244), does not bind to any T-MARE(β) base.

In contrast to the MafB/c-Fos/T-MARE(β) complex, the protein-DNA interactions observed in the homodimeric $MafB_2$/T-MARE complex are almost identical in the two MafB protomers, reflecting the symmetric nature of the overall complex (Figures 2A and S2). Whereas interactions with the DNA phosphate backbone are distributed over the complete T-MARE, base-specific interactions by residues R244 and N248 are restricted to the G/C positions ±4 and ±5 of the two T-MARE-specific, extended three-base elements. Interestingly, no residues from the EHR are involved in any specific side-chain-mediated T-MARE interactions.

A comparative analysis of the protein interactions with the DNA phosphate backbone of the two complexes revealed that the majority of the residues contributing to these interactions are not conserved in MafB and c-Fos (Figure 3B). Two MafB residues, R243 and Y251, which contribute to DNA-backbone recognition of the extended T-MARE base triplet by hydrogen bonds, are substituted with small hydrophobic residues in c-Fos (I142, A150). Conversely, a c-Fos residue (R159) that binds to the phosphate group of one of the central TRE bases is replaced in MafB with a small hydrophobic amino acid (V260) that does not have the ability to bind to DNA, thus shifting the overall layout of MafB-mediated DNA phosphate interactions toward the extended T-MARE base triplet. However, as the key MafB residues responsible for base-specific interactions are conserved in c-Fos (MafB/c-Fos, R244/R143, and N248/N147), our structural data indicate that the ability to form a different set of additional phosphate-mediated DNA backbone interactions, namely mediated by MafB-specific residues R243 and Y251, is an important parameter for the different preferred DNA recognition sequences by c-Fos and MafB, represented by TRE and the extended T-MARE half-sites, respectively. Together these structural data reveal the molecular basis of distinct DNA-binding site preferences for $MafB_2$ homodimers and MafB/c-Fos heterodimers.

Molecular Parameters Permitting Facultative $MafB_2$ and MafB/c-Fos Assembly

We next analyzed the structures of the $MafB_2$ and MafB/c-Fos complexes to identify the molecular parameters that determine homo- versus heterodimer formation. The overall coiled-coil arrangement in $MafB_2$ and MafB/c-Fos extends over six complete heptad repeats (Figure 4), generating extensive interface surfaces (1,275 $Å^2$ in $MafB_2$, 1,058 $Å^2$ in MafB/c-Fos). Most of the coiled-coil interactions are found within the four central heptad repeats II–V of both complexes, whereas the flanking repeats I and VI are more loosely arranged (Figures 4 and S3). In both protein assemblies, most of the specificity-determining interactions are found in repeats II, III, and V.

Repeat position *d* in the first four repeats of MafB is a highly conserved leucine, which is the most common amino acid in this position in canonical coiled coils (Miller, 2009). However, in repeat V, it is occupied by an unusual aromatic amino acid (Y294). In the homodimeric $MafB_2$ complex, the phenyl side chains of the same residue from the two MafB helices point away from each other (Figure 4C). In each of the MafB repeats I, II, and V, position *a* is represented by positively charged residues, which is rare in other bZip coiled coils. Two of these residues contribute to the two salt-bridge pairs of the $MafB_2$ homodimer, along with negatively charged residues from neighboring *g* positions: E269–K270 (heptad II) and E290–R291 (heptad V).

Surprisingly and in marked contrast to most other coiled-coil arrangements in bZip transcription factors (Miller, 2009; Vinson et al., 2006), there are no specific interactions between any residues from heptad positions *e* and *g*. These observations suggest that many of the heptad interactions found in the homodimeric MafB leucine zipper are specific for MafB and deviate from the type of interactions found in other bZip transcription factors. This finding is further supported by a comparison of the $MafB_2$/T-MARE complex with a recent structure of protein/DNA complex of MafG (Figures S4A–S4C; Kurokawa et al., 2009), which is member of the related family of small Maf

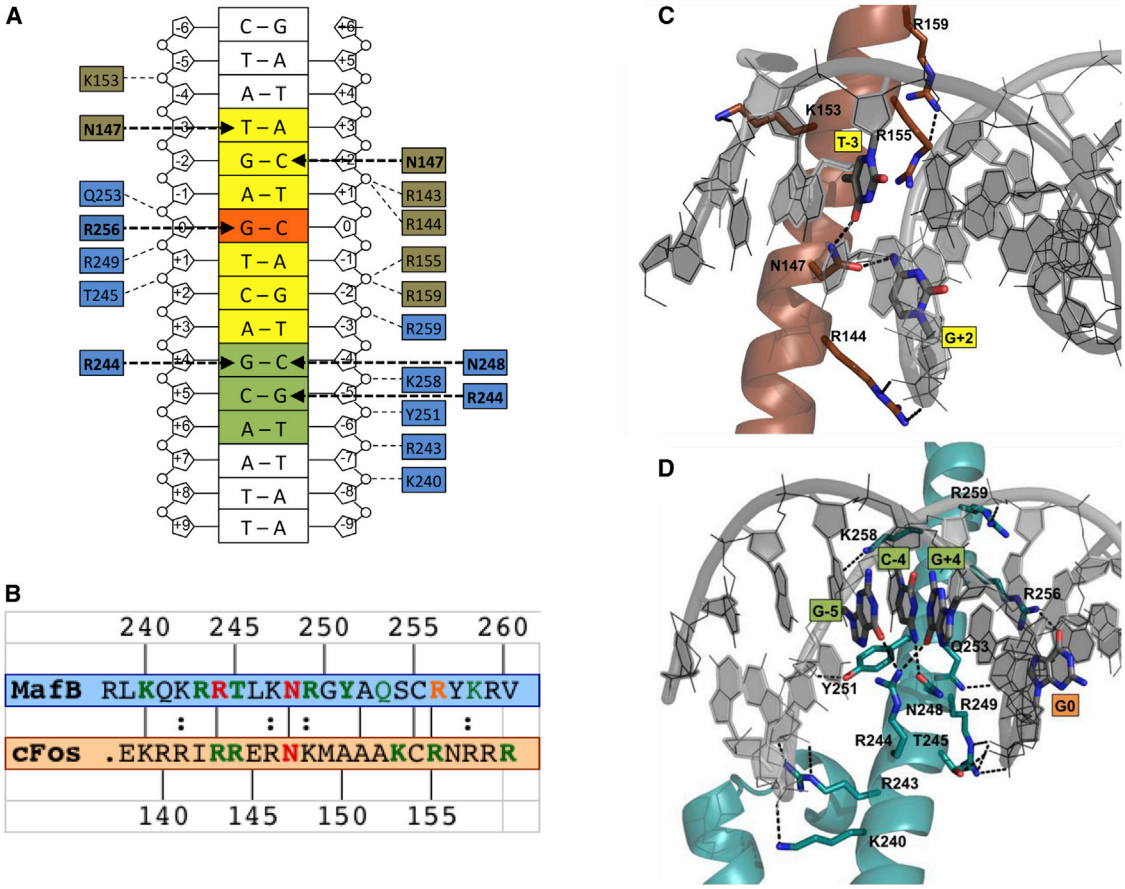

Figure 3. Protein-DNA Interactions in the Heterodimeric MafB/c-Fos/T-MARE(β) Complex

Color codes are as in Figure 1; oxygen and nitrogen atoms are in red and blue, respectively.

(A) Schematic representation, highlighting base-specific interactions in bold and remaining hydrogen-bond interactions in regular characters. Hydrogen bonds are indicated with dashed arrows.

(B) Structure-based sequence alignment of the BR from MafB and c-Fos. Residues involved in base-specific interactions, red; residues involved in interactions with the phosphate backbone of T-MARE or T-MARE(β), green.

(C and D) Ribbon representation emphasizing (C) c-Fos/DNA interactions and (D) MafB/DNA interactions. The second protein partner is shown in gray in each presentation. The view of (C) is similar to that shown in Figure 2. The view of (D) is rotated by about 180° with respect to (C) and Figure 2, to allow complete visualization of protein/DNA interactions. Dashed lines indicate hydrogen bonds; contributing protein residues and nucleotides are labeled. For reasons of clarity, additional van-der-Waals interactions are not indicated.

transcription factors that shares the same domain structure responsible for coiled-coil-mediated protein-protein assembly and DNA binding, but lacks a transactivation domain (Eychène et al., 2008). Although the interface positions (*a*, *d*, *e*, and *g*) of the coiled-coil region from MafB and MafG share 50% sequence identity (12/24 residues from six heptads), only one specific interaction—E269–K270 in MafB—is structurally conserved, whereas all further coiled-coil interaction pairs are specific either for MafG or MafB. Another structure of MafA (Lu et al., 2012), a member of the long Maf family, was not included into this comparison since many amino acid side chains in the leucine zipper region were only partially built.

In the c-Fos heptad repeat sequence, all *d* positions are represented by leucine residues. Positions *a* of repeats III and V, similar to our observations in MafB, are positively charged residues. K176 (c-Fos) from the *a* position of repeat III forms an additional hydrogen bond with Q276 (MafB) from the preceding *g* position, which is not observed in the $MafB_2$ coiled coil. However, in homodimeric $MafB_2$ such an interaction is not possible, as heptad III is the only one with a small hydrophobic residue (V277) in the respective *a* position (Figures 4C and 4D).

However, as each of the *a* positions in repeat V of MafB and c-Fos contains a positively charged residue and the *g* positions from the preceding heptad are represented by a glutamate, a pair of salt bridges—E290 (MafB)–K190 (c-Fos) and R291 (MafB)–E189 (c-Fos)—is formed that is in a virtually identical position to the symmetric pair of salt bridges E290–R291 in the $MafB_2$ coiled coil. For the other symmetric salt-bridge pair in the homodimeric $MafB_2$ assembly, E269–K270, only one of the two equivalent c-Fos residues is a charged residue (E168), and so only one salt bridge can be formed in the heterodimeric MafB/c-Fos coiled coil: E168 (c-Fos)–K270 (MafB). Thus, the total number of specific salt-bridge interactions from residues of heptad positions *a* and *g* in the heterodimeric MafB/c-Fos

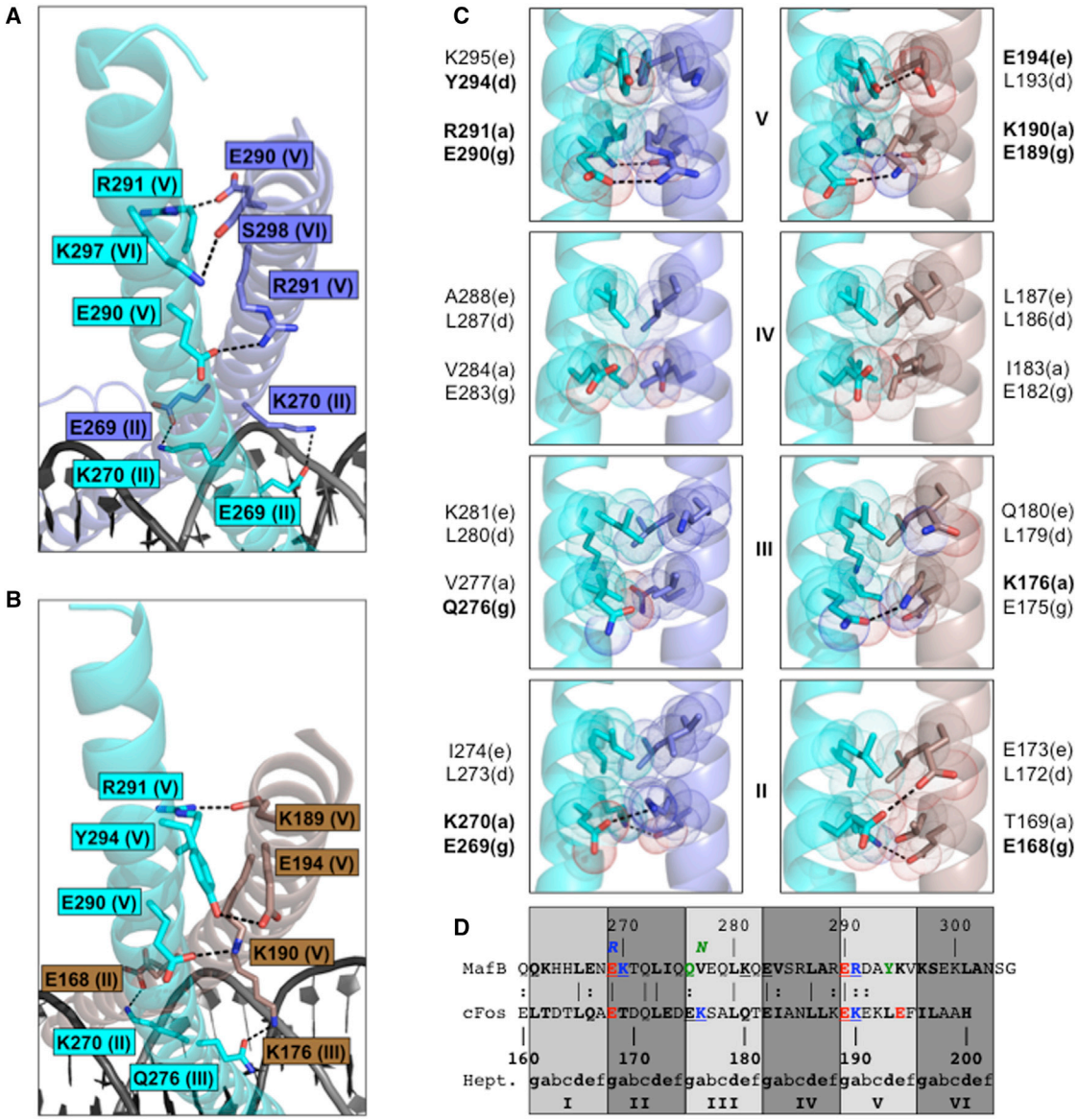

Figure 4. Comparison of Coiled-Coil Interactions in Homodimeric MafB$_2$ and Heterodimeric MafB/c-Fos

(A–C) Ribbon presentation of (A) MafB$_2$ and (B) MafB/c-Fos coiled-coil interactions. (C) Zoom into coiled-coil interactions of central heptads II, III, IV, and V, indicating the two-layered structure in each heptad. Side-chains of residues of positions *a* and *g* (first layer) and positions *d* and *e* (second layer) are shown by sticks and dot representation. Residue identities of MafB (left panels) and c-Fos (right panels) are indicated (bold, when involved in specific hydrogen-bond interactions in one or both of the two protein/DNA complexes). Color codes in (A)–(C) are as in Figure 2. Residues that are in potential hydrogen bond distances are connected with dashed lines.

(D) Structure-based sequence alignment of heptads I–VI. Negatively, positively, and uncharged polar residues involved in specific coiled-coil interactions are colored in red, blue, and green, respectively. Residues that are involved in specific heptad interactions are underlined. MafB mutants E269R and V277N are indicated.

complex is four, like in the homodimeric MafB$_2$ complex. Of these, three are structurally conserved in both bZip assemblies. Like in the homodimeric MafB$_2$ complex, no single, specific interaction between positions *e* and *g* is found in the heterodimeric MafB/c-Fos complex. In addition, an unusual specific interaction is formed between Y294 (MafB) from position *d* in heptad V and E194 (c-Fos) from position *e* in heptad V.

A comparison of the specific heptad interactions found in the c-Fos/MafB/T-MARE(β) and in the c-Fos/c-Jun/TRE complexes (Glover and Harrison, 1995) directly demonstrates a significantly larger number of interactions by heptad positions *a–g* and *e–g* in the latter assembly (Figures S4E and S4F). In contrast to bZip complexes with extended MARE-type DNA recognition specificities (MafB, MafG), in the c-Fos/c-Jun complex there are no predictable specific interactions missing (Grigoryan et al., 2009; Newman and Keating, 2003). None of the five identified heptad interactions from the *e–g* positions in the c-Fos/c-Jun complex is found in the heterodimeric c-Fos/MafB complex. Since the

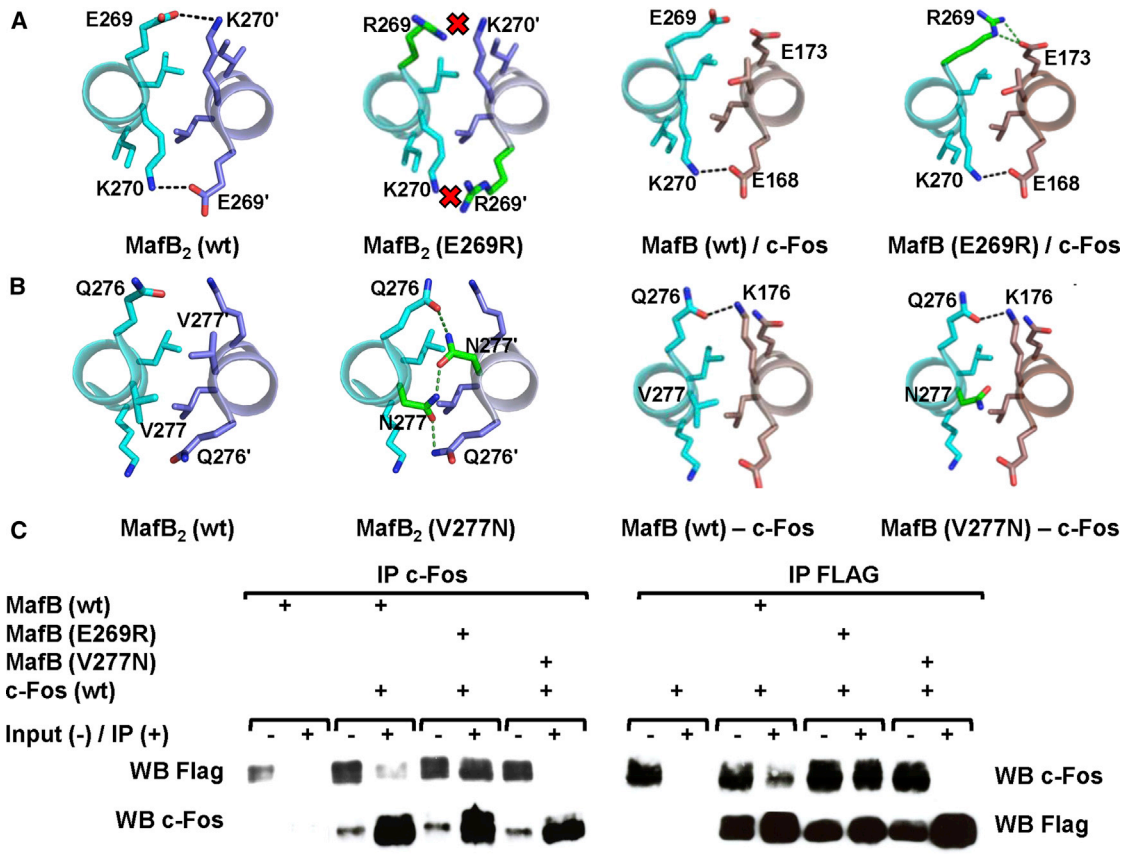

Figure 5. Design and Experimental Validation of Heterodimer (E269R)- and Homodimer (V277N)-Promoting MafB Versions

(A and B) Structural models of MafB mutant (A) E269R and (B) V277N (cf. Figure 4), based on the homodimeric $MafB_2$/T-MARE(α) complex (left) and the MafB/c-Fos/ T-MARE(β) complex (right). The models have been generated with the software PyMOL (http://www.pymol.org) and the most common side chain rotamer of each mutated residue is shown. A predicted repulsive arrangement of two positively charged residues, R269 and K270, of the MafB (E269R) mutant in the $MafB_2$ homodimer arrangement, emphasized by a red cross, and a predicted attractive interaction between R269 of the MafB (E269R) mutant and E173 from c-Fos in the MafB/c-Fos heterodimer arrangement are indicated. The view is from the N terminus to the C terminus in each heptad. Hydrogen bonds are indicated by dashed lines (experimental structures, black; mutant models, dark green). Color codes are as in Figure 2, except carbon atoms of mutated residues are green. (C) Differential interaction of MafB (wt), MafB (E269R), and MafB (V277N) with c-Fos in macrophages. Flag-tagged wt or MafB mutants were expressed together with c-Fos in MafB-deficient Maf-DKO macrophages (Aziz et al., 2009). Protein interactions were analyzed by immunoprecipitation of c-Fos followed by Western blot detection of MafB (left panel) or immunoprecipitation of MafB followed by Western blot detection of c-Fos (right panel).

DNA-binding preferences for c-Fos/c-Jun and c-Fos/MafB are different, proper heterodimeric bZip assembly involving c-Fos via the underlying specific coiled-coil interactions permits selective recognition of specific cognate DNA motifs.

Designed MafB Mutants with Altered Dimerization Properties and DNA-Binding Profile

We used this precise knowledge about the molecular parameters that support distinct $MafB_2$ and MafB/c-Fos dimerization in the presence of different MARE variants to design structure-based MafB mutants with altered dimerization preferences. To engineer a MafB version that is expected to favor heterodimerization with c-Fos, at the expense of the ability for homodimerization, we mutated E269 from the *g* position in heptad II into an arginine. We predicted that this MafB version would generate a repulsive interaction between K270 and the additional positive charge introduced in residue 269, and therefore that it would lose the ability to form the specific homodimeric salt-bridge interaction observed in the $MafB_2$ complex (Figures 4A, 4C, and 5A). As the residue equivalent to K270 in MafB is replaced by a threonine in c-Fos (Figure 4D), we reasoned that this mutation should have no negative effect on heterodimeric MafB/c-Fos complex formation. By contrast, we predicted that the E269R mutant could engage in an attractive interaction with E173 of c-Fos in the MafB/c-Fos heterodimer. Our prediction that the MafB (E269R) mutant would favor heterodimeric MafB/c-Fos assembly was confirmed by coimmunoprecipitation data showing an increased ability of the mutant to interact with c-Fos (Figure 5C). Furthermore, EMSA analysis revealed that even at a 16-fold excess of MafB over c-Fos, this mutant could still mediate heterodimer formation and, at equimolar ratios, resulted in almost exclusive MafB/c-Fos complex formation with only trace amounts of the homodimeric $MafB_2$. This is in contrast to the wild-type (wt) protein that does not form heterodimers in the presence of excess MafB and forms both types of complexes at equimolar ratios (Figure 6).

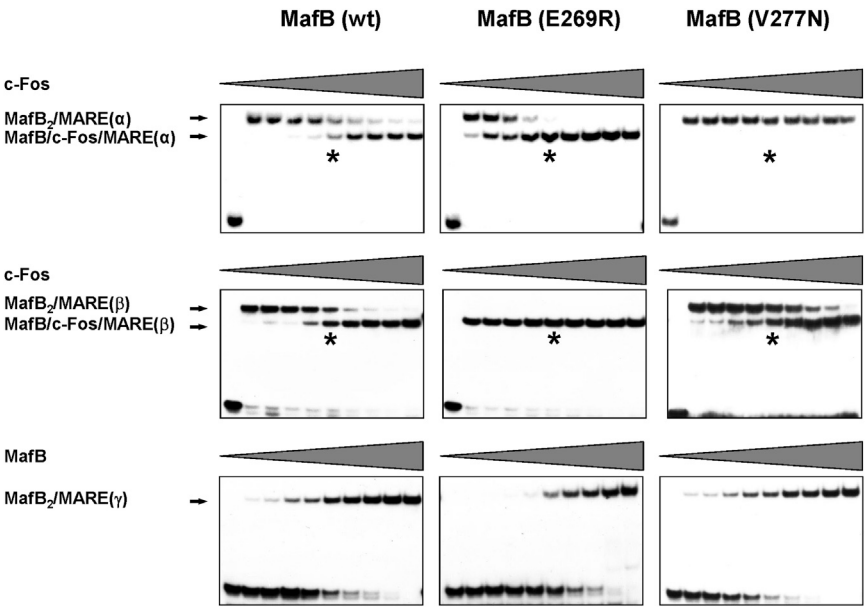

Figure 6. MARE Variant Binding Properties of MafB (E269R) and MafB (V277N) Mutants
EMSA assays of 4 pmol MafB (wt), MafB (V277N), or MafB (E269R) in the presence of increasing c-Fos concentrations (0, 0.25, 0.5, 1, 2, 4, 8, 16, 32, and 64 pmol, from left to right) on T-MARE(α) and T-MARE(β). Equimolar concentration of MafB and c-Fos is indicated by asterisk. The titrations on T-MARE(γ) were performed in absence of c-Fos, with increasing amounts (0.25, 0.5, 1, 2, 4, 8, 16, 32, and 64 pmol) of MafB (wt) or mutant proteins.

To engineer a MafB version with a preference for homodimerization, we mimicked known coiled coil bZip transcription factor assemblies that contain several glutamine/asparagine pairs with mixed donor/acceptor abilities of the two residues in neighboring *g* and *a* heptad positions (Schumacher et al., 2000). This type of residue pair allows the formation of a unique, stable assembly layer via a Q-N-N-Q hydrogen bond wire, maximizing the number of possible lateral hydrogen bonds per heptad repeat. Such an interaction is observed neither in the homodimeric $MafB_2$ assembly nor in the heterodimeric MafB/c-Fos complex. By mutating V277 of MafB into an asparagine, we designed such a motif allowing the formation of a Q276-N277-N277-Q276 hydrogen bond wire in the homodimeric $MafB_2$, but not in the heterodimeric MafB/c-Fos complex (Figure 5B). Consistent with a stabilization of homodimeric interactions, we expected this mutant to prefer homodimer rather than heterodimer formation under conditions in which both interactions are equally possible. This prediction was confirmed by coimmunoprecipitation experiments, in which MafB (V277N) showed stronger homodimerization preference than MafB (wt) protein (Figure 5C) and EMSA on a T-MARE, in which MafB (V277N) almost exclusively formed homodimers and no MafB/c-Fos complexes, even at a 20-fold excess of c-Fos (Figure 6). Taken together, this study shows that, by making use of structural leucine zipper interaction data, it is possible to alter the balance of homo- and heterodimeric MafB complexes in the presence of the same T-MARE sequence by introducing additional targeted attractive or repulsive interactions.

Based on our findings of altered homo- and heterodimeric assembly properties, we further investigated to what extent these MafB mutants could select for different T-MARE motifs. The MafB (E269R) variant indeed showed strong differential activity on T-MARE(γ)- and T-MARE(β)-binding sites. It required more than 10-fold higher concentrations than MafB (wt) to exhibit detectable binding as a homodimer to homodimer-promoting T-MARE(γ) (Figure 6) but showed exclusive heterodimer formation on heterodimer-promoting T-MARE(β), even at residual c-Fos concentrations (Figure 6). Consistent with this, in the presence of c-Fos, MafB (E269R) showed a 5-fold higher transactivation of a synthetic T-MARE(β) reporter construct than the wt protein and a reduced activity on a T-MARE(γ) reporter construct (Figure 7A). To test whether these observations would lead to a selective and preferential activation of T-MARE(β)-containing promoters when both MARE variant binding sites are available, we established a competitive transactivation assay with a T-MARE(γ)-promoter-driven Renilla luciferase reporter and a T-MARE(β)-promoter-driven Firefly luciferase reporter, which can be individually quantified in the same cell extract. When transfecting both reporters together with either MafB (wt) or MafB (E269R), we observed that MafB (wt) showed a strong preference for T-MARE(γ) promoter activation even in the presence of c-Fos, whereas MafB (E269R) strongly selected for T-MARE(β) promoter activation. As c-Fos is present endogenously in the transfected cells (Figure S5), this effect was already observed with transfection of MafB (E269R) only and further increased upon cotransfection of exogenous c-Fos (Figures 7B and S5). Together these data indicate that a single amino acid variation in MafB can induce a strong shift from activating T-MARE(γ)- to T-MARE(β)-containing promoters, and thus select both negatively against MafB activity on T-MARE(γ) and positively for MafB activity on T-MARE(β) sites.

However, when we investigated the MafB (V277N) mutant (Figure 5B), we did not observe a comparable effect on preferential T-MARE(γ)-binding site selection (Figure 6), possibly because the T-MARE(γ) variant already strongly favors homodimer binding that may be difficult to further enhance. The binding of this MafB variant to the heterodimer-promoting T-MARE(β) site (Figure 6) was also unchanged. This finding was expected, as unlike the MafB (E269R) mutant, the MafB (V277N) mutant does not generate any predicted repulsive interactions in the MafB/c-Fos heterodimeric complex. This observation was further confirmed in transactivation assays, in which the MafB (V277N) mutant showed no significant difference to the wt protein on synthetic T-MARE(γ) and T-MARE(β) reporters (Figure 7C). Although the MafB (V277N) mutant shows preferential homodimer formation on bipotential T-MARE(α) sites that can equally accommodate $MafB_2$ homodimers and MafB/c-Fos heterodimers (Figure 6, top panels), it does not select for preferential

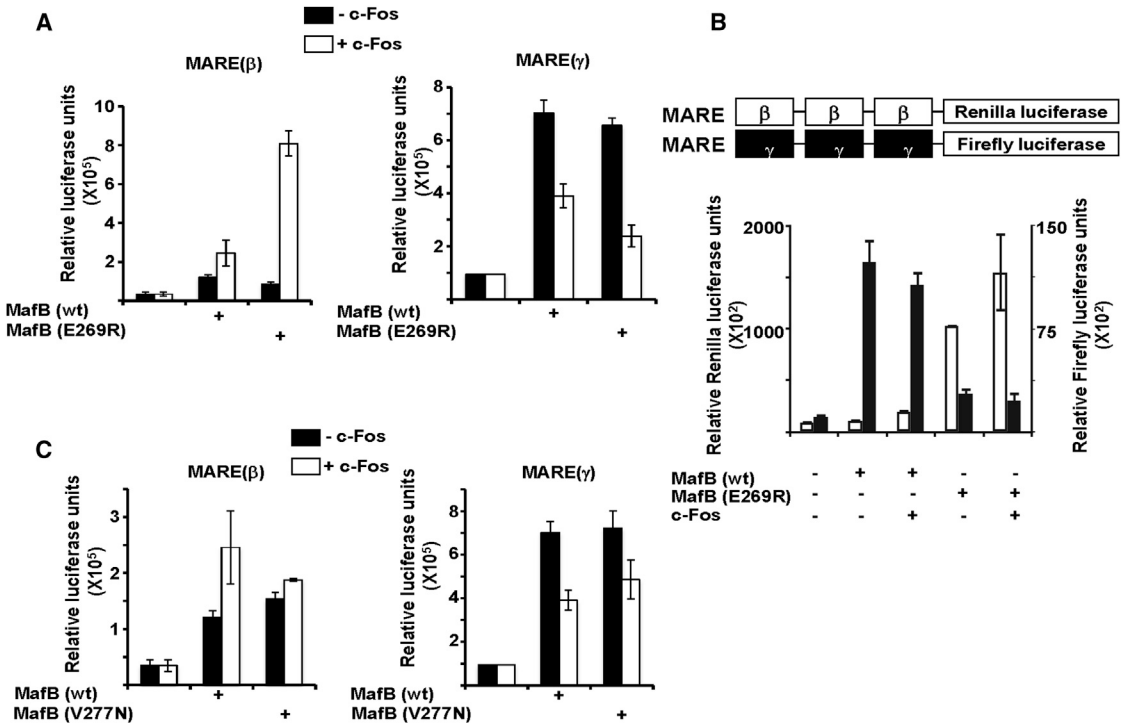

Figure 7. c-Fos-Dependent Transactivation Activity of MafB (wt), MafB (E269R), and MafB (V277N) on T-MARE(β) and T-MARE(γ) Sites
(A and B) Vectors for MafB (wt) or MafB (E269R) (A) or MafB (V277N) (B) expression were transfected in HEK293 cells line with multimerized MARE(β) (left) or MARE(γ) reporters (right) in the absence/presence of cotransfected exogenous c-Fos. Luciferase activity was measured 48 hr after transfection.
(C) Competitive transactivation assays of MafB (wt)/c-Fos and MafB (E269R)/c-Fos with T-MARE(γ)-Firefly- and T-MARE(β)-Renilla-luciferase reporters cotransfected in the same cells. Error bars correspond to SD.

binding to homodimer-promoting T-MARE(γ) sites versus heterodimer-promoting T-MARE(β) sites.

Perspectives

During recent years, regulated systems for gene transcription have been increasingly employed to alter genetic programs and associated functional readouts, such as signaling and metabolic pathways (Kiel et al., 2010; Lim, 2010; Tigges and Fussenegger, 2009). In this contribution, we show that, using two structures of the same bZip transcription factor MafB either assembled as a homodimer or as a heterodimer with another bZip transcription factor c-Fos, it is possible to change the balance of $MafB_2$ homodimer and MafB/c-Fos heterodimer formation on the same T-MARE sequence by targeted mutations in the respective leucine zippers. We also show that it is possible to change the binding preference for different T-MARE variants, as shown for the MafB (E269R) mutant. In general terms, our findings thus could provide innovative tools to control specific gene expression by selectively activating homo- or heterodimer-specific binding repertoires and signaling pathways. As the basic principles of coiled-coil protein/protein interactions are common to all bZip transcription factors, our procedures could be applicable to other members of this transcription factor family, to the extent that the DNA-recognition motifs of partner bZip transcriptions factors differ. Engineered MafB dimerization may ultimately enable the precise understanding and controlled manipulation of distinct activity states and binding repertoires of MafB, in particular in macrophages, with therapeutic potential in infectious disease, inflammatory or autoimmune disorders, regeneration, and tumor biology.

EXPERIMENTAL PROCEDURES

$MafB_2$/T-MARE and MafB/c-Fos/T-MARE(β) Purification and Crystallization

The C-terminal region of MafB from *Mus musculus* (residues 211–305; C298S) was purified as previously described (Textor et al., 2007). Homodimeric $MafB_2$ complexes were dialyzed overnight into 30 mM Tris-HCl (pH 7.3), 80 mM NaCl, 50 mM $MgCl_2$, and 3 mM β-mercaptoethanol at room temperature in the presence of an oligonucleotide encompassing the T-MARE-binding site (sequences in Table S1). The protein-DNA complex was further purified by size exclusion chromatography on a Superdex-75 (16/60) column (GE), equilibrated with the dialysis buffer. The pooled peak fractions corresponding to the $(MafB)_2$/T-MARE complex were analyzed by SDS-PAGE and native PAGE gels and concentrated to 5 mg/mL, using a centrifugal concentrator with a polyethersulfone membrane with a 10,000 molecular weight cut off (MWCO; VIVASPIN, Sartorius Stedim Biotech). Crystallization drops of 400 nL volume, using a 1:1 protein/mother liquor ratio, were set up in 96-well sitting-drop plates and allowed to equilibrate at 19°C. Diffracting crystals grew in the presence of 0.1 M Na-citrate (pH 5.0), 15% (w/v) polyethylene glycol (PEG)-4000, 5% (v/v) PEG-400, and 0.1 M $MgCl_2$.

For structural investigations of heterodimeric MafB/c-Fos complexes, a c-Fos fragment from *Mus musculus* (residues 138–200), encompassing the BR and Zip segment, was cloned in the pET-M11 vector and expressed in the *Escherichia coli* strain BL21(DE3)RIL. Cell pellets with overexpressed MafB and c-Fos were lysed separately under denaturing conditions in 4 M urea, 20 mM Tris-HCl (pH 7.5), 150 mM NaCl, and 15 mM β-mercaptoethanol.

The proteins were separately purified on a nickel nitrilotriacetic acid affinity column (QIAGEN). The heterodimer was refolded upon dialysis against a buffer containing 150 mM NaCl, 15 mM Tris (pH 7.5), and 10 mM dithiothreitol, in the presence of the chemically synthesized cognate DNA duplex T-MARE(β) (sequences in Table S1) and the tobacco etch virus protease in a mass ratio of 1:25 to remove the hexa-histidine tag. The MafB/c-Fos/T-MARE(β) complex was further purified by exclusion chromatography on a Superdex 75 column, equilibrated with the same buffer. Finally, the MafB/c-Fos/T-MARE(β) complex was concentrated up to 15 mg/mL, using a centrifugal concentrator with a polyethersulfone membrane with a 10,000 MWCO (VIVASPIN, Sartorius Stedim Biotech). Hanging drop crystallization trials were carried out at 20°C, by mixing equal volumes of reservoir solution and MafB/c-Fos/T-MARE(β) complex solution. Crystals grew from 0.075 M 4-(2-hydroxyethyl)-1-piperazineethanesulfonic-acid-Na (pH 7.5), 0.6 M sodium dihydrogen phosphate, 0.6 M potassium dihydrogen phosphate, 25% (v/v) glycerol.

MafB mutants were generated with the QuikChange Site-Directed Mutagenesis Kit (Stratagene). Primers of 45 bp were designed to introduce single mutations in MafB. MafB mutants were expressed and purified as the wt protein.

X-Ray Structure Determination

$MafB_2$/T-MARE

Crystals were cryoprotected by briefly soaking them into a solution used for crystallization, which included in addition 20% (w/v) PEG-400. A native X-ray data set was collected to a resolution of 2.9 Å on beamline ID23-2 at the European Synchotron Radiation Facility (ESRF) in Grenoble, France. The data were processed in the orthorhombic Laue group P222 with the XDS package (Kabsch, 2010). The structure was solved by molecular replacement in space group $P22_12_1$ with the program PHASER (McCoy, 2007), applying the coordinates of one MafB protomer (residues 212–253) bound to the CRE-like MARE (C-MARE) half-site from the $MafB_2$/C-MARE complex (Protein Data Bank accession number 4AUW) as the search model. The remaining protein residues and the DNA bases were built manually using the program COOT (Emsley and Cowtan, 2004) and successive cycles of restrained refinement with the program REFMAC5 (Murshudov et al., 1997). One cycle of simulated annealing was applied to the built model using the program PHENIX (Adams et al., 2011). The atomic coordinates were further refined to a final R_{work} and R_{free} of 23.5% and 27.5%, respectively, using a noncrystallographic symmetry restraint (Table 1). Ordered solvent molecules were added to the protein model, using the program ARP/wARP (Laskowski et al., 1998). The quality of the homodimeric MafB structure was validated using the program PROCHECK (Laskowski et al., 1993).

MafB/c-Fos/T-MARE(β)

All crystals used for X-ray data collection were mounted from the mother liquor onto a cryo-loop (Hampton Research) and directly flash-cooled under the nitrogen beam at 100K. X-ray data were collected on the synchrotron radiation beamlines BW7A and X11 at the DORIS III ring at EMBL/DESY in Hamburg, Germany. Experimental phases were determined from an X-ray data set to a maximum resolution of 3.2 Å, using the single-wavelength anomalous dispersion technique. For this purpose, crystals were derivatized with iodine using the vaporizing-iodine-labeling technique (Miyatake et al., 2006), by placing a small drop of 0.67 M KI/0.47 M I_2 solution next to the crystallization drop for 6 hr. The protein was weakly derivatized by this process, which together with the anomalous scattering from the DNA phosphate backbone provided sufficient phasing information by the identification of a total of 24 heavy atom sites to solve the structure using a combination of SHELX and SHARP programs (Bricogne et al., 2003; Schneider and Sheldrick, 2002). In addition, a native data set of the MafB/c-Fos/T-MARE(β) complex was collected to a resolution of 2.1 Å. The data set was processed with MOSFLM (Leslie and Powell, 2007) and programs of the CCP4 suite (CCP4, 1994). Further X-ray data collection and experimental phasing statistics are listed in Table 1.

Phase-extension was used to combine the experimentally determined phases with a high-resolution (2.3 Å) native data set. The final model was built with COOT (Emsley and Cowtan, 2004) and refined with the program REFMAC5 (Murshudov et al., 1997) to a final R_{work} and R_{free} of 22.8% and 25.6%, respectively. The asymmetric unit contains one MafB/c-Fos/DNA complex. The statistics of the structure refinement are summarized in Table 1. The stereochemical quality of the model was assessed by use of the program PROCHEK (Laskowski et al., 1993).

In the structure of the $MafB_2$/T-MARE complex, all DNA bases and the complete polypeptide chains, except one terminal residue of one of the two MafB molecules (F211) are visible. In the structure of the MafB/c-Fos/T-MARE(β) complex, the complete T-MARE(β) motif as well as the complete c-Fos and MafB polypeptide chains are visible, except tree residues from the N terminus (F211-D213) and two residues from the C terminus (S304-G305) of the expressed MafB fragment. The coordinates of the $MafB_2$/MARE(α) and MafB/c-Fos/MARE(β) complexes have been deposited in the Protein Data Bank with respective accession numbers 2WTY and 2WT7.

EMSA

Double-stranded synthetic oligonucleotides corresponding to T-MARE(α), to T-MARE(β), and to T-MARE(γ) (sequences in Table S1) sites were incubated with Klenow fragment DNA polymerase in the presence of [α^{32}P]CTP and purified on Qiaquick Spin Columns (QIAGEN). For c-Fos titration in presence of a constant amount of MafB, increasing amounts (0.25, 0.5, 1, 2, 4, 8, 16, 32, and 64 pmol) of recombinant c-Fos and recombinant protein (4 pmol) of MafB (wt) or MafB (E269R) and MafB (V277N) mutants were incubated with 0.05 ng of probe in 20 μl of binding reaction buffer (20 mM Tris-HCl [pH 7.5], 100 mM KCl, 0.1 mM EDTA, 5% glycerol, 0.1% Triton X-100, 0.02% BSA, 0.5 mg poly d[I-C]) for 20 min. For MafB titration in absence of c-Fos, increasing amounts (0.25, 0.5, 1, 2, 4, 8, 16, 32, and 64 pmol) of wt or mutant MafB proteins were incubated with 0.05 ng of probe in 20 μl of binding reaction buffer. Complexes formed were resolved on a 6% polyacrylamide (acrylamide/bisacrylamide ratio, 29:1) nondenaturating gel (Bio-Rad) in 0.5% Tris-glycine. Gels were dried and autoradiographed at −80°C.

Coimmunoprecipitation

MafB-deficient Maf double knockout (DKO) macrophages (Aziz et al., 2009) were transduced with indicated combinations of empty, c-Fos and MafB (wt), or MafB (E269R) and MafB (V277N) mutant encoding pMSCV vector using previously described infection protocols (Aziz et al., 2009). Cells were lysed in RIPA buffer (50 mM Tris-HCl [pH 8], 150 mM NaCl, 1% NP-40, 0.5% sodium deoxycholate, 0.1% SDS, protease inhibitors) and incubated for 30 min at 4°C. After clearing by centrifugation, lysates were incubated with the Flag-M2 antibody conjugated to agarose (Sigma, F2426) or with the anti-c-Fos antibody (Santa Cruz, sc-7202), previously coupled with protein A/G. After incubation, pellets were collected by centrifugation and washed four times in washing buffer (50 mM Tris-HCl [pH 8], 150 mM NaCl, protease inhibitors). Bound proteins were eluted with 62.5 mM Tris-HCl (pH 6.8), 2% SDS, 10% glycerol, and 0.002% bromophenol blue. Western blot detection was done by standard methods using anti-c-Fos (Santa Cruz, sc-7202) or anti-Flag-horseradish-peroxidase conjugated antibody (Sigma, A8592), respectively.

Transient Transfection and Reporter Gene Assay

Human embryonic kidney 293 (HEK293) cells were grown in Dulbecco's modified Eagle's medium supplemented with 10% fetal bovine serum in six-well plates to reach 60%–80% confluence at the time of transfection. DNA was transfected by calcium phosphate precipitation procedure as previously described (Sieweke et al., 1996). pTK81 luciferase reporter constructs (200 ng; Promega) containing three multimerized T-MARE(α), T-MARE(β), or T-MARE(γ) (sequences in Table S1) were cotransfected with 200 ng of pRc/CMV (Invitrogen) constructs driving the expression of wt, and mutant full-length MafB with or without 200 ng of pRc/CMV construct driving the expression of c-Fos or no transgene (vector control). Assays were performed in duplicate. The transfection efficiency was normalized by assaying for β-galactosidase activity from a cotransfected pCMV-LacZ construct, and luciferase activity was analyzed as previously described (Sieweke et al., 1996). For the competitive luciferase assay, Firefly luciferase gene downstream of T-MARE(γ) was excised using the BglII and XbaI sites and has been replaced by the Renilla luciferase gene. A total of 100 ng of pTK81-T-MARE(β)-Firefly and 100 ng of pTK81-T-MARE(γ)-Renilla were cotransfected with 200 ng of pRc/CMV or 200 ng of pRc/CMV-3X-Flag-MafB expression vector or with both MafB and c-Fos expression vector (200 ng each) by phosphate calcium precipitation. The transfection efficiency was normalized, by assaying for β-galactosidase activity from a cotransfected pCMV-LacZ construct, and luciferase activity was analyzed using a dual-luciferase reporter assay system

kit (Promega, catalog number E1910) according to the manufacturer's recommendations.

SUPPLEMENTAL INFORMATION

Supplemental Information includes Supplemental Experimental Procedures, five figures, and one table and can be found with this article online at http://dx.doi.org/10.1016/j.str.2013.12.017.

AUTHOR CONTRIBUTIONS

The experimental work was carried out by V.P., L.C.T., and L.V. S.J.H. contributed to X-ray structural analysis. The manuscript was written by M.W., with significant contributions by V.P., L.C.T., and M.H.S. M.H.S. and M.W. conceived, coordinated, and supported the project.

ACKNOWLEDGMENTS

We thank the staff of ESRF for assistance and support in using beamline ID23-2. This work was supported by the European Commission grant SPINE2-COMPLEXES (LSHG-CT-2006-031220). M.W. and M.H.S. were supported by the Volkswagen Stiftung (I/79 994-996). M.H.S. was supported by the Foundation pour la Recherche Médicale (DEQ20071210559 and DEQ20110421320), the Agence nationale de la Recherche (ANR-11-BSV3-0026), and the Association pour la Recherche sur le Cancer (ARC, 1131). M.H.S. is an INSERM-Helmholtz group leader. L.V. received fellowships from the Ministère de l'Enseignement Supérieur et de la Recherche and the ARC.

Received: August 13, 2013
Revised: November 30, 2013
Accepted: December 30, 2013
Published: February 13, 2014

REFERENCES

Adams, P.D., Afonine, P.V., Bunkóczi, G., Chen, V.B., Echols, N., Headd, J.J., Hung, L.W., Jain, S., Kapral, G.J., Grosse Kunstleve, R.W., et al. (2011). The Phenix software for automated determination of macromolecular structures. Methods *55*, 94–106.

Amit, I., Garber, M., Chevrier, N., Leite, A.P., Donner, Y., Eisenhaure, T., Guttman, M., Grenier, J.K., Li, W., Zuk, O., et al. (2009). Unbiased reconstruction of a mammalian transcriptional network mediating pathogen responses. Science *326*, 257–263.

Aziz, A., Soucie, E., Sarrazin, S., and Sieweke, M.H. (2009). MafB/c-Maf deficiency enables self-renewal of differentiated functional macrophages. Science *326*, 867–871.

Bricogne, G., Vonrhein, C., Flensburg, C., Schiltz, M., and Paciorek, W. (2003). Generation, representation and flow of phase information in structure determination: recent developments in and around SHARP 2.0. Acta Crystallogr. D Biol. Crystallogr. *59*, 2023–2030.

CCP4 (Collaborative Computational Project, Number 4) (1994). The CCP4 suite: programs for protein crystallography. Acta Crystallogr. D Biol. Crystallogr. *50*, 760–763.

Emsley, P., and Cowtan, K. (2004). Coot: model-building tools for molecular graphics. Acta Crystallogr. D Biol. Crystallogr. *60*, 2126–2132.

Eychène, A., Rocques, N., and Pouponnot, C. (2008). A new MAFia in cancer. Nat. Rev. Cancer *8*, 683–693.

Glover, J.N., and Harrison, S.C. (1995). Crystal structure of the heterodimeric bZIP transcription factor c-Fos-c-Jun bound to DNA. Nature *373*, 257–261.

Grigoryan, G., and Keating, A.E. (2008). Structural specificity in coiled-coil interactions. Curr. Opin. Struct. Biol. *18*, 477–483.

Grigoryan, G., Reinke, A.W., and Keating, A.E. (2009). Design of protein-interaction specificity gives selective bZIP-binding peptides. Nature *458*, 859–864.

Hai, T., and Curran, T. (1991). Cross-family dimerization of transcription factors Fos/Jun and ATF/CREB alters DNA binding specificity. Proc. Natl. Acad. Sci. USA *88*, 3720–3724.

Introna, M., Hamilton, T.A., Kaufman, R.E., Adams, D.O., and Bast, R.C., Jr. (1986). Treatment of murine peritoneal macrophages with bacterial lipopolysaccharide alters expression of c-fos and c-myc oncogenes. J. Immunol. *137*, 2711–2715.

Kabsch, W. (2010). Xds. Acta Crystallogr. D Biol. Crystallogr. *66*, 125–132.

Kataoka, K., Fujiwara, K.T., Noda, M., and Nishizawa, M. (1994). MafB, a new Maf family transcription activator that can associate with Maf and Fos but not with Jun. Mol. Cell. Biol. *14*, 7581–7591.

Kerppola, T.K., and Curran, T. (1994a). A conserved region adjacent to the basic domain is required for recognition of an extended DNA binding site by Maf/Nrl family proteins. Oncogene *9*, 3149–3158.

Kerppola, T.K., and Curran, T. (1994b). Maf and Nrl can bind to AP-1 sites and form heterodimers with Fos and Jun. Oncogene *9*, 675–684.

Kiel, C., Yus, E., and Serrano, L. (2010). Engineering signal transduction pathways. Cell *140*, 33–47.

Koga, K., Takaesu, G., Yoshida, R., Nakaya, M., Kobayashi, T., Kinjyo, I., and Yoshimura, A. (2009). Cyclic adenosine monophosphate suppresses the transcription of proinflammatory cytokines via the phosphorylated c-Fos protein. Immunity *30*, 372–383.

Kurokawa, H., Motohashi, H., Sueno, S., Kimura, M., Takagawa, H., Kanno, Y., Yamamoto, M., and Tanaka, T. (2009). Structural basis of alternative DNA recognition by Maf transcription factors. Mol. Cell. Biol. *29*, 6232–6244.

Kusunoki, H., Motohashi, H., Katsuoka, F., Morohashi, A., Yamamoto, M., and Tanaka, T. (2002). Solution structure of the DNA-binding domain of MafG. Nat. Struct. Biol. *9*, 252–256.

Laskowski, R.A., Moss, D.S., and Thornton, J.M. (1993). Main-chain bond lengths and bond angles in protein structures. J. Mol. Biol. *231*, 1049–1067.

Laskowski, R.A., MacArthur, M.W., and Thornton, J.M. (1998). Validation of protein models derived from experiment. Curr. Opin. Struct. Biol. *8*, 631–639.

Leslie, A.G.W., and Powell, H.R. (2007). Processing diffraction data with MOSFLM. In Evolving Methods for Macromolecular Crystallography, R.J. Read and J.L. Sussman, eds. (Dordrecht, The Netherlands: Springer), pp. 41–51.

Lim, W.A. (2010). Designing customized cell signalling circuits. Nat. Rev. Mol. Cell Biol. *11*, 393–403.

Lu, X., Guanga, G.P., Wan, C., and Rose, R.B. (2012). A novel DNA binding mechanism for maf basic region-leucine zipper factors inferred from a MafA-DNA complex structure and binding specificities. Biochemistry *51*, 9706–9717.

McCoy, A.J. (2007). Solving structures of protein complexes by molecular replacement with Phaser. Acta Crystallogr. D Biol. Crystallogr. *63*, 32–41.

Miller, M. (2009). The importance of being flexible: the case of basic region leucine zipper transcriptional regulators. Curr. Protein Pept. Sci. *10*, 244–269.

Miyatake, H., Hasegawa, T., and Yamano, A. (2006). New methods to prepare iodinated derivatives by vaporizing iodine labelling (VIL) and hydrogen peroxide VIL (HYPER-VIL). Acta Crystallogr. D Biol. Crystallogr. *62*, 280–289.

Murshudov, G.N., Vagin, A.A., and Dodson, E.J. (1997). Refinement of macromolecular structures by the maximum-likelihood method. Acta Crystallogr. D Biol. Crystallogr. *53*, 240–255.

Newman, J.R., and Keating, A.E. (2003). Comprehensive identification of human bZIP interactions with coiled-coil arrays. Science *300*, 2097–2101.

Ogata, K., Sato, K., and Tahirov, T.H. (2003). Eukaryotic transcriptional regulatory complexes: cooperativity from near and afar. Curr. Opin. Struct. Biol. *13*, 40–48.

Panne, D. (2008). The enhanceosome. Curr. Opin. Struct. Biol. *18*, 236–242.

Pulendran, B., Tang, H., and Manicassamy, S. (2010). Programming dendritic cells to induce T(H)2 and tolerogenic responses. Nat. Immunol. *11*, 647–655.

Reményi, A., Schöler, H.R., and Wilmanns, M. (2004). Combinatorial control of gene expression. Nat. Struct. Mol. Biol. *11*, 812–815.

Sarrazin, S., Mossadegh-Keller, N., Fukao, T., Aziz, A., Mourcin, F., Vanhille, L., Kelly Modis, L., Kastner, P., Chan, S., Duprez, E., et al. (2009). MafB restricts M-CSF-dependent myeloid commitment divisions of hematopoietic stem cells. Cell *138*, 300–313.

Schneider, T.R., and Sheldrick, G.M. (2002). Substructure solution with SHELXD. Acta Crystallogr. D Biol. Crystallogr. *58*, 1772–1779.

Schumacher, M.A., Goodman, R.H., and Brennan, R.G. (2000). The structure of a CREB bZIP.somatostatin CRE complex reveals the basis for selective dimerization and divalent cation-enhanced DNA binding. J. Biol. Chem. *275*, 35242–35247.

Sieweke, M.H., and Graf, T. (1998). A transcription factor party during blood cell differentiation. Curr. Opin. Genet. Dev. *8*, 545–551.

Sieweke, M.H., Tekotte, H., Frampton, J., and Graf, T. (1996). MafB is an interaction partner and repressor of Ets-1 that inhibits erythroid differentiation. Cell *85*, 49–60.

Textor, L.C., Wilmanns, M., and Holton, S.J. (2007). Expression, purification, crystallization and preliminary crystallographic analysis of the mouse transcription factor MafB in complex with its DNA-recognition motif Cmare. Acta Crystallogr. Sect. F Struct. Biol. Cryst. Commun. *63*, 657–661.

Tigges, M., and Fussenegger, M. (2009). Recent advances in mammalian synthetic biology-design of synthetic transgene control networks. Curr. Opin. Biotechnol. *20*, 449–460.

Tillmanns, S., Otto, C., Jaffray, E., Du Roure, C., Bakri, Y., Vanhille, L., Sarrazin, S., Hay, R.T., and Sieweke, M.H. (2007). SUMO modification regulates MafB-driven macrophage differentiation by enabling Myb-dependent transcriptional repression. Mol. Cell. Biol. *27*, 5554–5564.

Vinson, C., Acharya, A., and Taparowsky, E.J. (2006). Deciphering B-ZIP transcription factor interactions in vitro and in vivo. Biochim. Biophys. Acta *1759*, 4–12.

Yamamoto, T., Kyo, M., Kamiya, T., Tanaka, T., Engel, J.D., Motohashi, H., and Yamamoto, M. (2006). Predictive base substitution rules that determine the binding and transcriptional specificity of Maf recognition elements. Genes Cells *11*, 575–591.